

Reversible single-crystal to single-crystal transformations in a Hg(II) derivative. 1D-polymeric chain \rightleftharpoons 2D-networking as a function of temperature†

Shaikh M. Mobin,^{a,b,c} Ashwini K. Srivastava,^{*c} Pradeep Mathur^{*a,b} and Goutam Kumar Lahiri^{*a,b}

Received 6th March 2010, Accepted 25th June 2010

DOI: 10.1039/c0dt00085j

Reactions of HgX_2 ($\text{X} = \text{Cl}^-$, Br^- , I^-) with the ligand hep-H (hep-H = 2-(2-hydroxyethyl)pyridine) in methanol at 298 K result in 1D-polymeric chains of $[(\text{X})\text{Hg}(\mu\text{-X})_2(\text{hep-H})]_n$, **1–3**, respectively, where hep-H binds to the Hg(II) ions in a monodentate fashion exclusively with the pyridine nitrogen donor and the suitably *ortho*-positioned $-(\text{CH}_2)_2\text{OH}$ group of hep-H remains pendant. The packing diagrams of **1–3** exhibit extensive intramolecular and intermolecular hydrogen bonding interactions leading to hydrogen bonded 2D network arrangement in each case. Though the single crystal of either **2** ($\text{X} = \text{Br}$) or **3** ($\text{X} = \text{I}$) loses crystallinity upon heating, the single crystal of **1** selectively transforms to a 2D-polymeric network, **4** on heating at 383 K for 1.5 h. The polymeric **4** consists of central dimeric $[\text{Hg}(\mu_3\text{-Cl})(\text{hep-H})\text{Cl}]_2$ units, which are covalently linked with the upper and lower layers of $[-(\mu\text{-Cl})_2\text{-Hg}-(\mu\text{-Cl})_2\text{-Hg}(\mu\text{-Cl})_2-]_n$. The packing diagram of **4** reveals the presence of O–H–Cl and C–H–Cl hydrogen bonding interactions which in effect yields hydrogen bonded 3D-network. Remarkably, the single crystals of **4** convert back to the single crystals of parent **1** on standing at 298 K for three days.

Introduction

Recent discoveries of single-crystal to single-crystal (SCSC) transformations at the discrete or polymeric molecular frameworks by vapour diffusion,¹ heat² or photolytic methods³ have evoked much research interest because of their potential applications in catalysis,⁴ designing of sensors⁵ and magnetic materials.⁶ This is primarily due to the in built structural rigidity of certain molecular frameworks, which can maintain crystallinity in spite of molecular reorganizations through severe bond breaking and forming processes at the single crystal level. For example, SCSC transformation of a Pt complex involving the reversible binding and subsequent liberation of SO_2 *via* bond formation and cleavage without losing its crystallinity has been established to be a convenient route for designing efficient gas storage devices.⁷ Similarly, the non-porous single-crystal of *p*-Bu-calix[4]arene shows the host–guest transportation properties at the SCSC level through weak van der Waals cooperative interactions between the molecular components.⁸ Therefore, the major challenge involved towards the SCSC process is to design single-crystals of suitable molecular frameworks, which can retain the crystallinity on exposure of external conditions such as heat or vapour or light during the transformation process in order to reach the thermodynamically stable structural form through internal

chemical and or physical changes. Solvent-free reaction conditions in SCSC processes are an added advantage particularly from the point of view of environmentally benign green chemistry.⁹ SCSC transformations, either at the polymeric or discrete level, are documented in the literature for several transition metal ions, Mn(II),¹⁰ Fe(III),¹¹ Co(II),¹² Ni(II),¹³ Cu(II),^{1b-c,e,2g,14} Zn(II),^{15,2e,3c} Cd(II),¹⁶ Ag(II),^{3d,3e,4a} Pb(II),^{2h,17} Pt(II),⁷ and lanthanides.¹⁸ There also exists one report of a SCSC transformation for a Hg derivative, an *irreversible* SCSC transformation of a hydrogen bonded dimeric Hg(II) complex, $[\text{Hg}_2(\mu\text{-bpd})\text{I}_4]$ (bpd = 1,4-bis-(2-pyridyl)-2,3-diaza-1,3-butadiene) to a 2D-networking by the application of heat.¹⁹ The SCSC processes reported in literature at the polymeric molecular frameworks have been associated with the following transformations: (i) the hydrogen bonded polymeric structures to the covalently bonded polymeric frameworks *via* the cleavage and reformation of multiple bonds,^{1a,2f,15b} (ii) adsorption–resorption of solvent molecules,^{1a,1e,9a,15a} and (iii) dehydration–rehydration of coordinated or lattice water molecules.^{1a,4a,11a,14a,17b}

The present article therefore originates from our recent interest^{1b-c} to design suitable molecular frameworks, which can exhibit reversible SCSC transformations. In this context we report here the synthesis and structural characterisation of 1D-coordination polymers of $[\text{Hg}(\mu\text{-X})_2(\text{hep-H})(\text{X})]_n$ (**1–3**) [hep-H = 2-(2-hydroxyethyl)pyridine]; $\text{X} = \text{Cl}$ (**1**), Br (**2**), I (**3**)] and the effect of heat on the single crystals of **1–3**. This leads to an unprecedented *reversible* SCSC transformation of Hg derivative selectively when $\text{X} = \text{Cl}$ (**1**): 1D-coordination polymeric chain in **1** transforms to a 2D-polymeric network in **4**, which reverts back to **1** as a function of temperature.

The Hg derivatives (**1–3**) have been selectively chosen for the present exploration as unlike other group 12 metal ions (Zn and Cd) the SCSC process involving the Hg derived species has so far been confined to only one irreversible process.¹⁹ To the best of our

^aNational Single-Crystal X-ray Diffraction Facility, IIT Bombay, Powai, Mumbai, 400076, India

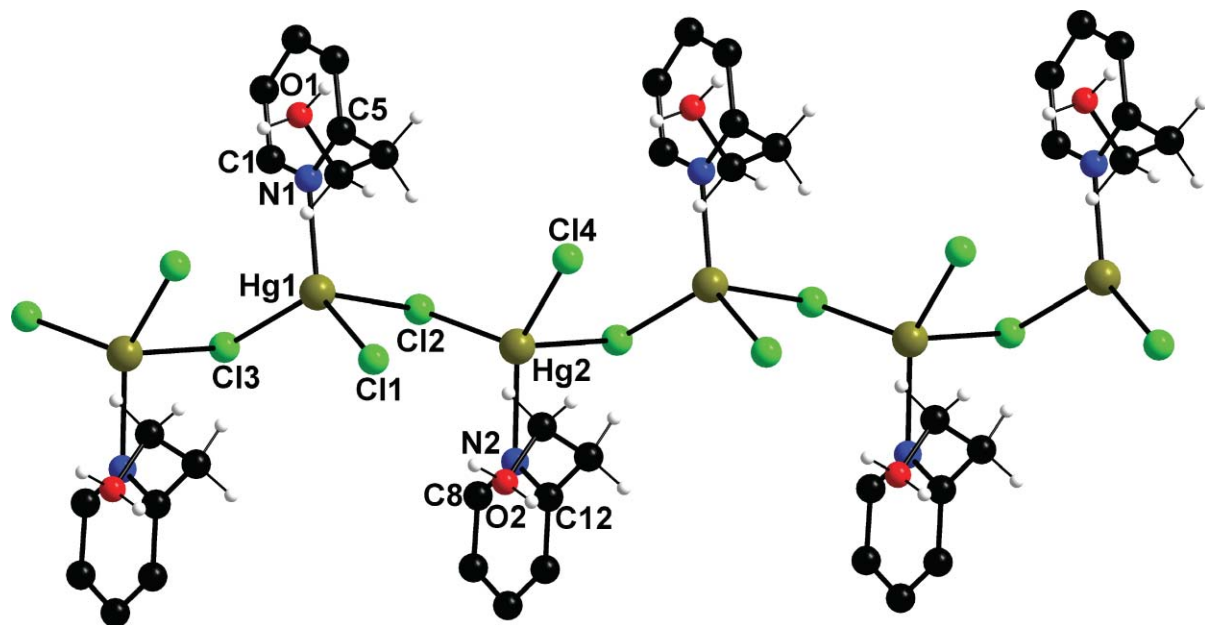
^bDepartment of Chemistry, IIT Bombay, Powai, Mumbai, 400076, India

^cDepartment of Chemistry, University of Mumbai, Vidyannagari, Mumbai, 400098, India

† Electronic supplementary information (ESI) available: Bond distances and angles; hydrogen bonding parameters; ORTEP figures; packing diagrams; TGA; PXRD; DSC. CCDC reference numbers 768937–768941. For ESI and crystallographic data in CIF or other electronic format see DOI: 10.1039/c0dt00085j

Table 1 Crystallographic data for 1–4

| | 1 (X = Cl) (150 K) | 2 (X = Br) (150 K) | 3 (X = I) (150 K) | 4 (150 K) | 1 (X = Cl) Regenerated (150 K) |
|---|---|---|--|---|---|
| Empirical formula | C ₁₄ H ₁₈ N ₂ O ₂ Cl ₄ Hg ₂ | C ₁₄ H ₁₈ N ₂ O ₂ Br ₄ Hg ₂ | C ₁₄ H ₁₈ N ₂ O ₂ I ₄ Hg ₂ | C ₇ H ₉ NOCl ₄ Hg ₂ | C ₁₄ H ₁₈ N ₂ O ₂ Cl ₄ Hg ₂ |
| Formula weight | 789.30 | 967.11 | 1155.11 | 666.13 | 789.30 |
| Crystal symmetry | Triclinic | Triclinic | Triclinic | Triclinic | Triclinic |
| Space group | $P\bar{1}$ | $P\bar{1}$ | $P\bar{1}$ | $P\bar{1}$ | $P\bar{1}$ |
| <i>a</i> /Å | 7.5938(2) | 7.8101(2) | 8.2332(2) | 7.4719(14) | 7.5737(11) |
| <i>b</i> /Å | 9.2613(2) | 9.3923(2) | 9.5688(2) | 9.6025(15) | 9.2458(10) |
| <i>c</i> /Å | 14.6635(3) | 14.8571(3) | 15.3779(3) | 9.6934(17) | 14.6588(13) |
| α /° | 102.200(2) | 101.709(2) | 101.358(2) | 75.965(14) | 102.113(8) |
| β /° | 104.045(2) | 102.871(2) | 99.013(2) | 78.872(15) | 103.806(10) |
| γ /° | 90.508(2) | 90.718(2) | 90.974(2) | 87.877(14) | 90.655(10) |
| <i>V</i> /Å ³ | 975.87(4) | 1038.44(4) | 1171.67(4) | 662.0(2) | 972.6(2) |
| <i>Z</i> | 2 | 2 | 2 | 2 | 2 |
| μ /mm ⁻¹ | 16.270 | 22.471 | 18.366 | 23.942 | 16.325 |
| <i>D_c</i> /mg m ⁻³ | 2.686 | 3.093 | 3.274 | 3.342 | 2.695 |
| <i>F</i> (000) | 720 | 864 | 1008 | 588 | 720 |
| Crystal size mm ³ | 0.33 × 0.26 × 0.21 | 0.23 × 0.18 × 0.14 | 0.28 × 0.23 × 0.18 | 0.30 × 0.26 × 0.21 | 0.24 × 0.23 × 0.19 |
| θ range/° | 3.29 to 32.87 | 3.24 to 32.73 | 3.33 to 32.80 | 3.46 to 32.63 | 3.29 to 33.29 |
| Reflections collected/unique | 11 023/6469 [<i>R</i> (int) = 0.0212] | 10 708/6765 [<i>R</i> (int) = 0.0551] | 13 453/7673 [<i>R</i> (int) = 0.0425] | 8766/4329 [<i>R</i> (int) = 0.0240] | 11 683/6339 [<i>R</i> (int) = 0.0904] |
| Data/restraints/parameters | 6469/0/221 | 6765/0/219 | 7673/0/219 | 4329/0/138 | 6334/13/216 |
| <i>R</i> ₁ , <i>wR</i> ₂ [<i>I</i> > 2σ(<i>I</i>)] | 0.0286, 0.0786 | 0.0618, 0.1760 | 0.0497, 0.1280 | 0.0423, 0.1097 | 0.0734, 0.2137 |
| <i>R</i> ₁ , <i>wR</i> ₂ (all data) | 0.0329, 0.0799 | 0.0754, 0.1824 | 0.0652, 0.1337 | 0.0656, 0.1160 | 0.0934, 0.2547 |
| GOF | 1.099 | 1.038 | 1.029 | 0.878 | 1.262 |
| Largest diffraction peak, hole/e Å ⁻³ | 2.901 and -2.296 | 5.270 and -5.650 | 3.897 and -3.656 | 2.248 and -3.209 | 5.750 and -10.174 |

**Fig. 1** Perspective view of the 1D-coordination polymeric chain in 1.

knowledge the present work demonstrates the first example of a reversible SCSC transformation involving the Hg derivative 1.

Results and discussion

The reaction of respective HgX₂ (X = Cl⁻, Br⁻, I⁻) with the ligand, 2-(2-hydroxyethyl)pyridine (hep-H) in a 1 : 1 molar ratio in methanol at 298 K directly results in the formation of colourless single crystals in each case corresponding to 1D-coordination polymeric chains of [(X)Hg(μ-X)₂(hep-H)]_n, 1–3. (Fig. 1, Table 1 and Fig. S1–S3, Tables S1–S2 (ESI).†

Compounds 1–3 crystallise in the triclinic $P\bar{1}$ space group with a crystallographically imposed inversion centre. The crystal structures of 1–3 reveal that they are isostructural: each consists of a Hg ion bonded to the N atom of a hep-H ligand as well as three halides. Such units are connected *via* bridging halides to give a zigzag polymeric chain in which the Hg ion exhibits distorted tetrahedral coordination geometry (3 halides, 1 nitrogen). The hep-H ligand in 1–3 is linked to the Hg ions only through the neutral pyridine nitrogen donor leaving the suitably *ortho*-positioned (CH₂)₂OH or (CH₂)₂O⁻ a potential pendant donor [Hg–O(hep-H) non-bonding distances are 4.64,

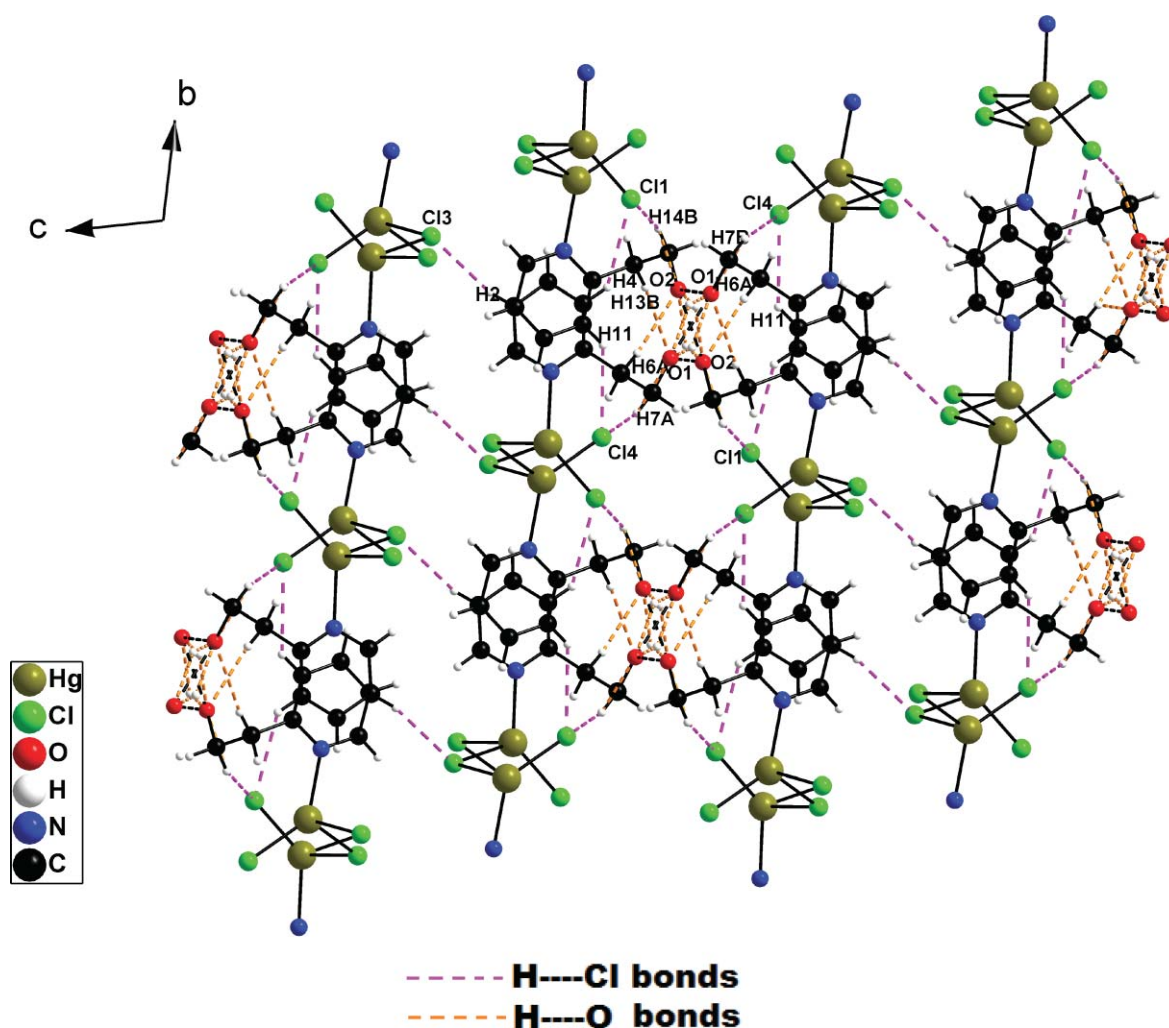
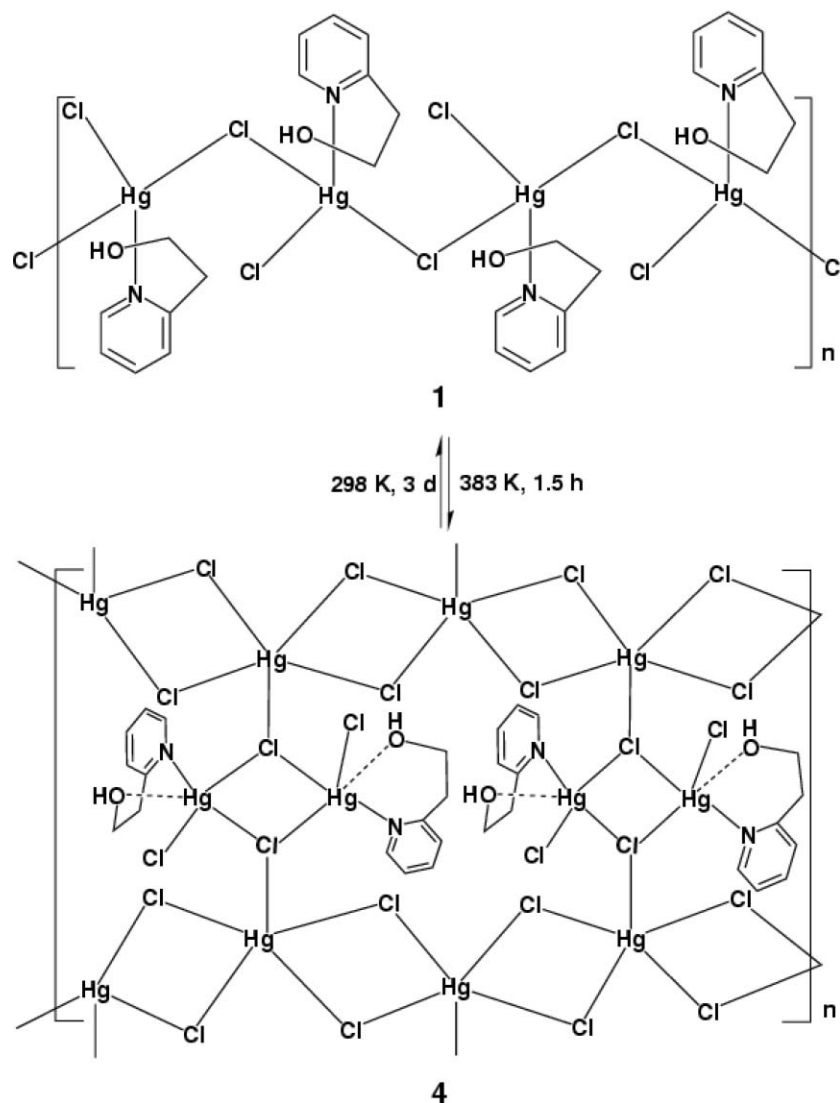


Fig. 2 Packing diagram of the hydrogen bonded 2D network in **1** along the *a*-axis.

4.71 and 4.94 Å in **1**, **2** and **3**, respectively] similar to that reported in the discrete monomeric *cis*-[PtCl₂(NH₃)(hep-H)]²⁰ and the dimeric [Ag₂(sac)₂(hep-H)₂]²¹ (sac = saccharinate) complexes. These contrast with other discrete molecular frameworks, as well as polymeric complexes, in which the hep⁻ ligand is specifically bonded as a monoanionic bidentate N, O⁻ donor.^{1b-c,22} The two coordinated hep-H ligands attached to the two adjacent Hg ions in **1–3** exist in *trans* configuration and the same pattern continues along the polymeric chain. The Hg–N (hep-H) distances in **1–3** vary slightly along the chain in the range of 2.222(4)–2.307(8) Å (Tables S1–S2).[†] The Hg–halide distances in each of **1–3** vary significantly *viz.*, Hg(1)–X(1), Hg(1)–X(2), and Hg(1)–X(3) (X = Cl/Br/I): 2.3630(10)/2.4815(11)/2.6428(6), 2.7858(10)/2.9324(10)/3.0824(6) and 2.4981(10)/2.5813(10)/2.7406(6) Å, respectively, (ESI, Tables S1–S2),[†] and while moving from one Hg centre to another Hg centre along the polymeric chain in **1–3** the same Hg–X distances again vary slightly (Hg(2)–X(2), Hg(2)–X(3), and Hg(2)–X(4) distances are 2.4986(10)/2.5879(10)/2.7553(6), 2.7533(10)/2.9064(10)/3.0591(6) and 2.3797(11)/2.4929(11)/2.6528(6) Å, respectively, (ESI, Tables S1–S2).[†]

The packing diagrams of analogous **1–3** reveal the presence of following intramolecular and complicated intermolecular

hydrogen bonding interactions (Fig. 2 and ESI, Fig. S4 and S5, Tables S3–S4).[†] (i) The intramolecular C–H···X²³ hydrogen bonding involves the interaction between one of the hydrogen atoms of the pendant β-CH₂ group (H7A and H14B) of hep-H ligands and terminal halide atoms (X4 and X1). (ii) The coordination polymeric layer of **1–3** is connected with the neighbouring upper and lower layers *via* intermolecular C–H···X hydrogen bonds between the hydrogen atoms of the pyridine ring of hep-H ligands in one layer to the terminal X1 and X4 atoms of upper and lower layers, respectively, along the *b*-axis. (iii) Furthermore, each layer is extended along the ± *c*-axis *via* O1–H01A···O2/O2–H02A···O1 interaction between the pendant hydroxyl groups of hep-H ligands in two adjacent layers. **1** shows C–H···Cl hydrogen bonding interaction between hydrogen atom of the pyridine ring of hep-H in one layer and the bridging Cl3 atom in the adjacent layer (Fig. 2) whereas in **2** and **3** the adjacent layers are interconnected *via* Br–Br and I–I short contacts (ESI, Fig. S4 and S5).[†] Moreover, C–H···O²⁴ hydrogen bonding interactions exist between hydrogen atoms of the pendant α-CH₂ group (H6A and H13B) and hydroxyl O atoms of hep-H ligands in two adjacent layers which in effect results in hydrogen bonded 2D network arrangement.



Scheme 1 Temperature dependant reversible SCSC transformations: 1D-chain (1) \rightleftharpoons 2D-network (4).

Single crystals of 1–3 were subjected to heating in order to explore the possibility of single-crystal to single-crystal (SCSC) transformations. Though the single crystals of 2 (X = Br) and 3 (X = I) lose crystallinity on heating, the single crystal of 1 undergoes a temperature dependant reversible transformation: 1D-chain (1) to 2D-network (4) at the SCSC level (Scheme 1).

On heating at 383 K over a period of 1.5 h, the single crystal of the 1D-polymeric chain of 1 undergoes a unique structural transformation leading to the formation of a 2D-network in 4 (Scheme 1, Fig. 3 and Table 1, and ESI Fig. S6 and Table S1).[†] However, the same transformation, 1 \rightarrow 4 can also occur at a lower temperature of 353 K but the heating needs to continue for a much longer period of time > 3 h. The single crystal of 4 possesses the triclinic $P\bar{1}$ space group with a crystallographically imposed inversion centre. The 2D-network in 4 consists of dimeric $[\text{Hg}(\mu_3\text{-Cl})(\text{hep-H})\text{Cl}]_2$ units, which are sandwiched between two layers of $[-(\mu\text{-Cl})_2\text{-Hg}-(\mu\text{-Cl})_2\text{-Hg}-(\mu\text{-Cl})_2-]_n$ (Scheme 1 and Fig. 3). The central dimeric $[\text{Hg}(\mu_3\text{-Cl})(\text{hep-H})\text{Cl}]_2$ units are linked with the upper and lower layers of $[-(\mu\text{-Cl})_2\text{-Hg}-(\mu\text{-Cl})_2\text{-Hg}-(\mu\text{-Cl})_2-]_n$ through the formation of covalent bonds between the $\mu\text{-Cl}$ groups

of the former and the Hg units of the latter leading to $\mu_3\text{-Cl}$ linkages. Unlike 1 (the separation between Hg and OH of hep-H: 4.64 Å) in 4 there is a weak Hg–OH(hep-H) interaction with Hg–OH distance of 2.834 Å.²⁵

In each dimeric $[\text{Hg}(\mu_3\text{-Cl})(\text{hep-H})\text{Cl}]_2$ unit, the Hg ion is in a distorted square pyramidal geometry with the basal positions occupied by the pyridine N and alcoholic OH (weakly bonded) atoms of the hep-H ligand, the terminal Cl and one of the bridging Cl ligands, while the second bridging Cl exists in the axial position. However, in the oligomeric units, $[-(\mu\text{-Cl})_2\text{-Hg}-(\mu\text{-Cl})_2\text{-Hg}-(\mu\text{-Cl})_2-]_n$, the penta-coordinated Hg ion exhibits a highly irregular geometry with four $\mu\text{-Cl}$ and one $\mu_3\text{-Cl}$ donors.

The packing diagram of 4 (Fig. 4 and ESI, Table S3)[†] reveals the presence of O–H \cdots Cl and C–H \cdots Cl hydrogen bonding interactions. The O1–H101 \cdots Cl4 interaction involves the hydrogen atom of the hydroxyl group of hep-H in the dimeric unit $[\text{Hg}(\mu_3\text{-Cl})(\text{hep-H})\text{Cl}]_2$ and one of the bridging Cl4 atoms of the oligomeric unit $[-(\mu\text{-Cl})_2\text{-Hg}-(\mu\text{-Cl})_2\text{-Hg}-(\mu\text{-Cl})_2-]_n$. The two C–H \cdots Cl hydrogen bonds, C(4)–H(4) \cdots Cl(1) and C(4)–H(4) \cdots Cl(3) are developed,

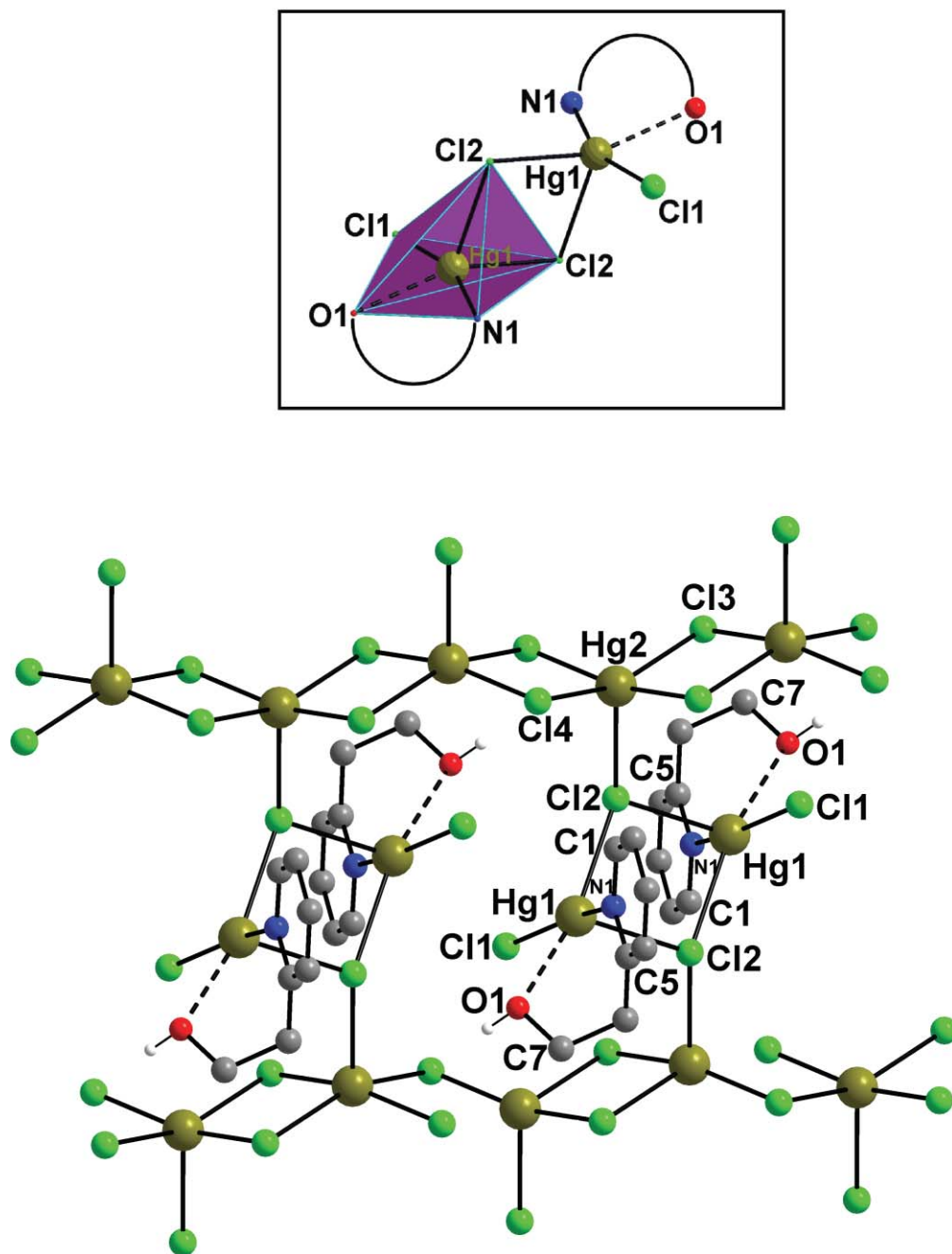


Fig. 3 Perspective view of the 2D-network in **4**. Inserts show the geometry of the central dimeric Hg-units in **4**.

respectively, *via* the interactions of the hydrogen atom (H4) of the pyridine ring of hep-H with the terminal chlorine atom Cl(1) of the central dimeric unit and with the bridging chloride atom (Cl3) of the oligomeric unit. Furthermore, the β -CH₂ group of hep-H of the central dimeric unit forms C7–H7B \cdots Cl4 hydrogen bonding interaction with the bridging Cl4 atom of the oligomeric unit, which eventually results in a hydrogen bonded 3D-network (Fig. 4).

The transformation of **1** to **4** formally involves a series of consecutive bond breaking and bond reforming steps. Although a detailed understanding of the mechanism is not available to us, a tentative pathway can be proposed (Scheme 2) based on a

closer look at the connectivities in **1** and **4**. Under the influence of heat, cleavage of alternate Hg–hep-H bonds in adjacent layers in **1** (A and B, Scheme 2) may take place, followed by (i) rotation of the layer A by about 180° and (ii) cleavage of the bridging Hg–Cl in the layer B, which in turn facilitate the formation of new covalent linkages, Hg–Cl between the two layers and Hg–OH(hep-H) (though weak interaction) in each layer in **4**, as depicted in Scheme 2. The early loss of one hep-H ligand is also supported by the TGA experiment of the bulk sample of **1** (ESI, Fig. S7).† The powder-XRD patterns of the isostructural **1** and **2** (ESI, Fig. S8)† are expectedly different from that of the transformed **4** (ESI, Fig. S9).†

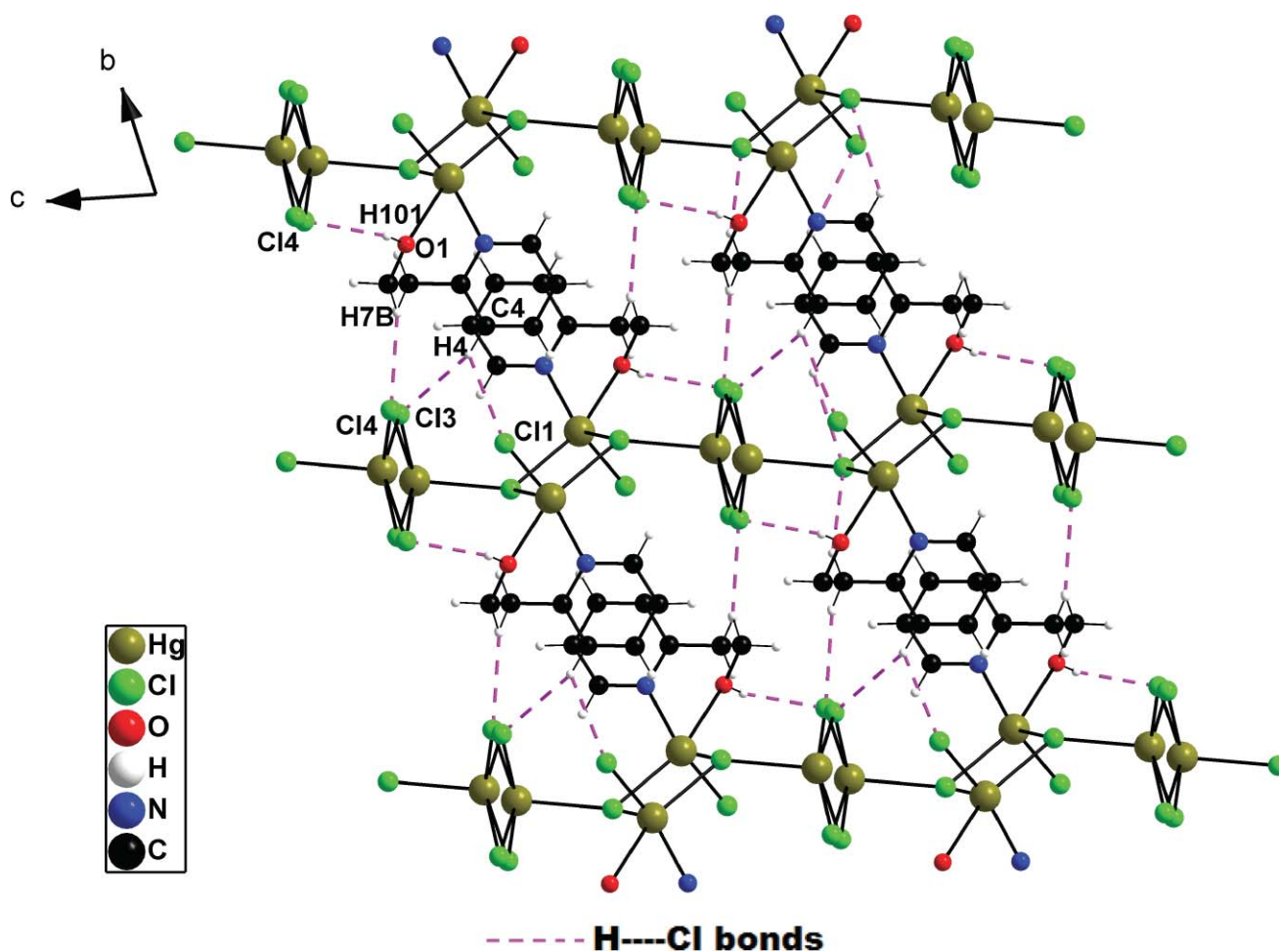


Fig. 4 Packing diagram of the hydrogen bonded 3D network in **4** along the *b*-axis.

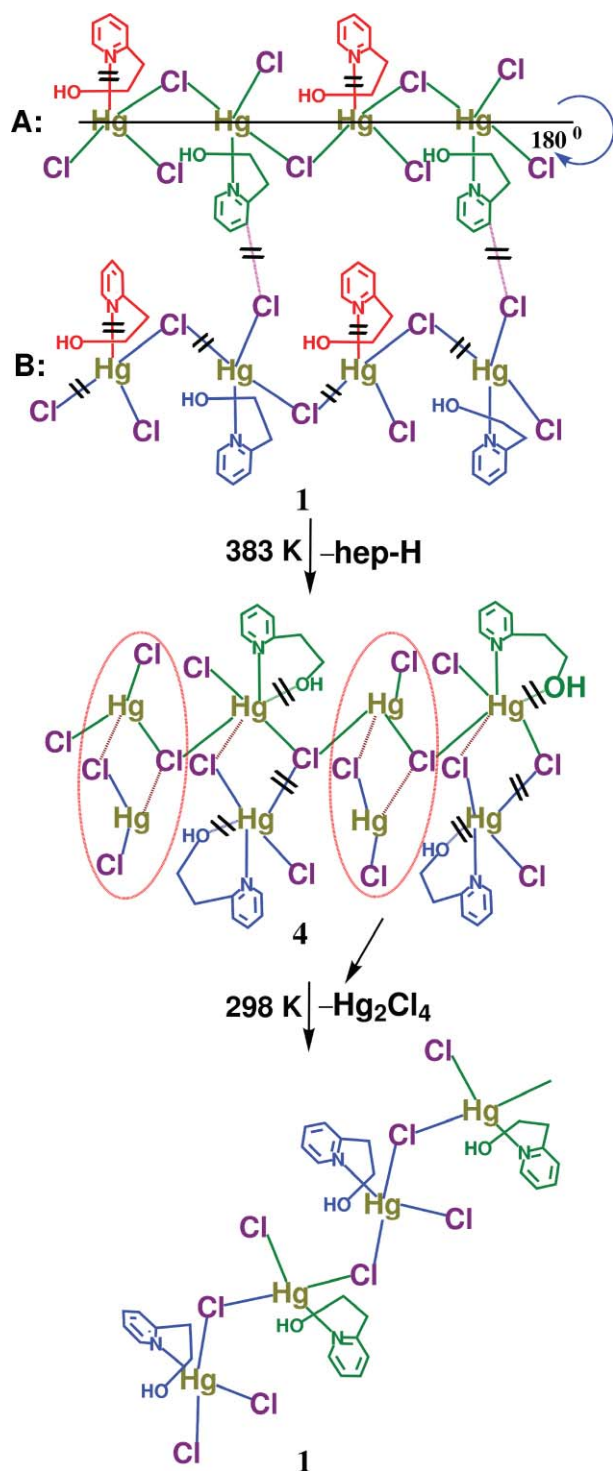
On allowing the single crystal of **4** to stand at 298 K over a period of three days it transforms back to the single crystal of **1**, as confirmed by the single-crystal X-ray structure of the regenerated **1** (Table 1 and ESI Fig. S10 and Table S1).† The reverse SCSC process, **4** → **1** also takes place through several chemical transformations and it appears to be associated with the net removal of the central Hg₂Cl₄ units in certain forms *via* the cleavage of the bridging Hg–Cl bonds (marked in circle, Scheme 2) and the cleavage of Hg–O(hep-H) weak interactions.

Differential scanning calorimetry (DSC) features of the complexes **1**(Cl) and **2**(Br) in the range of 273–523 K (0–250 °C) are shown in ESI, Fig. S11†, which exhibit a similar pattern of one endothermic peak at around 145 °C (~418 K) followed by two distinct but close by exothermic peaks at around 160 °C (~433 K). Though the relatively higher net enthalpy change (ΔH) associated with **2** (–285.8 J g^{–1}) as compared to **1** (–209.2 J g^{–1}) thermodynamically also favours the phase transition process in **2**, unlike the single crystal of **1**, the single crystal of **2** fails to maintain the necessary crystallinity on heating, which indeed retards the SCSC transformation to occur like in **1**. The DSC feature of the transformed product **4** shows multiple close by exothermic processes around 190 °C (ESI, Fig. S11).† The slower SCSC

transformation process of **4** to **1** (3 d at 298 K, Scheme 1) has not been featured in the DSC experiment.

Conclusions

The present work demonstrates the following salient features: (i) an unprecedented *reversible* single-crystal to single-crystal (SCSC) transformation involving the Hg derived co-ordination polymeric complex leading to 1D-coordination polymeric chain in **1** ⇌ 2D-network in **4** as a function of temperature. (ii) Though the single crystals of 1D-coordination polymeric frameworks in the precursor complexes, **1**(Cl), **2**(Br) and **3**(I) are equally stable at 298 K irrespective of the nature of the halides, on heating, rather surprisingly, it is only the single crystal of **1**, with Cl[–] ligands, which retains the necessary crystallinity, and undergoes the SCSC transformation to the 2D-polymeric network of **4** and subsequently the backward SCSC process *i.e.* **4** → **1** takes place on cooling the single crystal at 298 K for 3 d. (iii) The transformations of **1** ⇌ **4** are associated with complex molecular reorganization processes at either direction primarily through simultaneous multiple covalent bond breaking and bond reforming steps. (iv) A tentative interpretation regarding the molecular transformations associated with **1** → **4** as well as **1** ← **4** has been extended.



Scheme 2 Proposed pathways for the transformations of **1** \rightarrow **4** (slice of the hydrogen bonded network in **1** is considered, Fig. 2) and the reverse process of **4** \rightarrow **1**. \approx : Bond cleavage, $—$: new bond formation.

Experimental

Materials

The commercially available starting materials, HgCl_2 , HgBr_2 , HgI_2 , 2-(2-hydroxyethyl)pyridine (hep-H) and reagent grade solvents: methanol were used as received.

Physical measurements

Elemental analyses were carried out with a Perkin-Elmer 240C elemental analyser. DTA/TGA experiments were done on a Perkin Elmer Instrument. X-ray (powder) diffraction data were collected on a Philips X'Pert Pro X-ray diffraction system using monochromated $\text{Cu-K}\alpha_1$ radiation ($\lambda = 1.5406 \text{ \AA}$). DSC experiments were carried out by using Dupont (model 2000, USA) instrument.

Preparation of $[(\text{X})\text{Hg}(\mu\text{-X})_2(\text{hep-H})]_\infty$ [$\text{X} = \text{Cl}^-$ (1**), Br^- (**2**), I^- (**3**)].** The polymeric complexes **1–3** were prepared by following a general procedure. Details are given below for **1**.

A solution of hep-H (123 mg, 1 mmol) in methanol (25 cm^3) was added to a solution of HgCl_2 (272 mg, 1 mmol) in methanol (25 cm^3) and the resultant solution was stirred magnetically for 6 h at 298 K. The solution was then passed through the filter paper (Whatman filter paper, 70 mm) in order to remove any unreacted materials. The filtrate was then allowed to stand at 298 K for crystallisation. On slow evaporation of the solvent, colourless single crystals of **1** were obtained after 10 d. Mp: 205–207 °C. Yield: 215 mg (80%). Anal. calcd For $\text{C}_{14}\text{H}_{18}\text{N}_2\text{O}_2\text{Cl}_4\text{Hg}_2$, ($M_r = 789.30$): C 21.27, H 2.30, N 3.55. Found: C 21.69, H 2.41, N 3.66. TGA: temperature range °C (% weight loss): 95–200 (18.0) corresponds to loss of one hep-H ligand; 205–405 (70) corresponds to HgCl_2 .

2: Mp: 209–211 °C. Yield: 185 mg (51%). Anal. calcd for $\text{C}_{14}\text{H}_{18}\text{N}_2\text{O}_2\text{Br}_4\text{Hg}_2$, ($M_r = 967.11$): C 17.40, H 1.88, N 2.90. Found: C 17.45, H 1.91, N 2.96.

3: Mp: 215–217 °C. Yield: 205 mg (45%). Anal. calcd for $\text{C}_{14}\text{H}_{18}\text{N}_2\text{O}_2\text{I}_4\text{Hg}_2$, ($M_r = 1155.11$): C 14.51, H 1.57, N 2.42. Found: C 14.49, H 1.51, N 2.46.

SCSC-transformation of $[(\text{Cl})\text{Hg}(\mu\text{-Cl})_2(\text{hep-H})]_\infty$ (1**) to **4**.** A colourless single crystal of **1** was exposed to heating at 383 K for 1.5 h. Subsequently, the crystal was subjected to X-ray analysis, which confirmed the identity of the crystal as **4**. The bulk sample of **4** was prepared by heating several single crystals of **1** at 383 K for 1.5 h. Mp: 257–259 °C. Anal. calcd for $\text{C}_7\text{H}_8\text{N}_2\text{OCl}_4\text{Hg}_2$, ($M_r = 665.12$): C 12.61, H 1.21, N 2.10. Found: C 12.69, H 1.29, N 2.16

Backward SCSC-transformation of **4 to $[(\text{Cl})\text{Hg}(\mu\text{-Cl})_2(\text{hep-H})]_\infty$ (**1**).** Single-crystal of **4** was allowed to stand at 298 K for three days and the crystal was then subjected to X-ray diffraction data collection which confirmed the regeneration of the starting $[\text{Hg}(\mu\text{-Cl})_2(\text{hep-H})]_\infty$ (**1**). The bulk sample of the regenerated **1** was then prepared by allowing the several single crystals of **4** to stand at 298 K for 3 d. Mp: 205–207 °C. Anal. calcd for $\text{C}_{14}\text{H}_{18}\text{N}_2\text{O}_2\text{Cl}_4\text{Hg}_2$, ($M_r = 789.30$): C 21.27, H 2.30, N 3.55. Found: C 21.63, H 2.37, N 3.63.

Crystal structure determination

Single-crystal X-ray structural studies of **1–4** and **1**-regenerated were performed on a CCD Oxford Diffraction XCALIBUR-S diffractometer equipped with an Oxford Instruments low-temperature attachment. Data were collected at 150(2) K using graphite-monochromated $\text{Mo-K}\alpha$ radiation ($\lambda_{\alpha} = 0.71073 \text{ \AA}$). The strategy for the data collection was evaluated by using the CrysAlisPro CCD software. The data were collected by the standard phi-omega scan techniques, and were scaled and reduced

using CrysAlisPro RED software. The structures were solved by direct methods using SHELXS-97²⁶ and refined by full matrix least squares with SHELXL-97, refining on F^2 . The positions of all the atoms were obtained by direct method. All non-hydrogen atoms except N2 atom were refined anisotropically. The hydrogen atoms were placed in geometrically constrained positions and refined with isotropic temperature factor, generally $1.2 \times U_{eq}$ of their parent atoms. The disordered hydrogen atoms associated with the pendant hydroxyl groups in **1–3** and **1**-regenerated are split over two positions. All the H-bonding interactions, mean plane analyses, and molecular drawings were obtained using the Diamond ver. 3.1 and ORTEP program. The selective crystal and refinement data, bond distances and bond angles and hydrogen bond parameter are summarized in Table 1 and ESI, Tables S1–S4.†

Acknowledgements

Financial support received from the Department of Science and Technology (New Delhi, India) is gratefully acknowledged. Important suggestions extended by Dr V. G. Puranik, Center for Materials Characterization, National Chemical Laboratory, Pune-411008, India, is gratefully acknowledged.

References

- (a) J. J. Vittal, *Coord. Chem. Rev.*, 2007, **251**, 1781; (b) M. M. Shaikh, A. K. Srivastava, P. Mathur and G. K. Lahiri, *Inorg. Chem.*, 2009, **48**, 4652; (c) M. M. Shaikh, A. K. Srivastava, P. Mathur and G. K. Lahiri, *Dalton Trans.*, 2010, **39**, 1447; (d) S. Supriya and S. K. Das, *J. Am. Chem. Soc.*, 2007, **129**, 3464; (e) A. K. Sah and T. Tanase, *Chem. Commun.*, 2005, 5980.
- (a) V. Niel, A. L. Thompson, M. C. Muoz, A. Galet, A. E. Goeta and J. A. Real, *Angew. Chem., Int. Ed.*, 2003, **42**, 3760; (b) X.-N. Cheng, W.-X. Zhang and X.-M. Chen, *J. Am. Chem. Soc.*, 2007, **129**, 15738; (c) J. D. Ranford, J. J. Vittal, D.-Q. Wu and X.-D. Yang, *Angew. Chem., Int. Ed.*, 1999, **38**, 3498; (d) L. Iordanidis and M. G. Kanatzidis, *J. Am. Chem. Soc.*, 2000, **122**, 8319; (e) J. J. Vittal and X.-D. Yang, *Cryst. Growth Des.*, 2002, **2**, 259; (f) C. Hu and U. Englert, *Angew. Chem., Int. Ed.*, 2005, **44**, 2281; (g) T. K. Maji, G. Mostafa, R. Matsuda and S. Kitagawa, *J. Am. Chem. Soc.*, 2005, **127**, 17152; (h) A. Aslani and A. Morsali, *Chem. Commun.*, 2008, 3402.
- (a) N. L. Toh, M. Nagarathinam and J. J. Vittal, *Angew. Chem., Int. Ed.*, 2005, **44**, 2237; (b) X. Ouyang, F. W. Fowler and J. W. Lauher, *J. Am. Chem. Soc.*, 2003, **125**, 12400; (c) G. S. Papaefstathiou, Z. Zhong, L. Geng and L. R. MacGillivray, *J. Am. Chem. Soc.*, 2004, **126**, 9158; (d) M. Nagarathinam and J. J. Vittal, *Angew. Chem., Int. Ed.*, 2006, **45**, 4337; (e) Q. Chu, D. C. Swenson and L. R. MacGillivray, *Angew. Chem., Int. Ed.*, 2005, **44**, 3569.
- (a) J.-P. Zhang, Y.-Y. Lin, W.-X. Zhang and X.-M. Chen, *J. Am. Chem. Soc.*, 2005, **127**, 14162; (b) Y. Kim and D. P. Jung, *Inorg. Chem.*, 2000, **39**, 1470.
- (a) L. Pan, H. Liu, X. Lei, X. Huang, D. H. Olson, N. J. Turro and J. Li, *Angew. Chem., Int. Ed.*, 2003, **42**, 542; (b) T. Sawaki and Y. Aoyama, *J. Am. Chem. Soc.*, 1999, **121**, 4793.
- (a) M. P. Suh, H. R. Moon, E. Y. Lee and S. Y. Jang, *J. Am. Chem. Soc.*, 2006, **128**, 4710; (b) H. J. Choi and M. P. Suh, *J. Am. Chem. Soc.*, 2004, **126**, 15844.
- M. Albrecht, M. Lutz, A. L. Spek and G. van Koten, *Nature*, 2000, **406**, 970.
- J. L. Atwood, L. J. Barbour, A. Jerga and B. L. Schottel, *Science*, 2002, **298**, 1000.
- P. T. Anastas and M. M. Kirchoff, *Acc. Chem. Res.*, 2002, **35**, 686.
- (a) M. C. Das and P. K. Bharadwaj, *J. Am. Chem. Soc.*, 2009, **131**, 10942; (b) W. Kaneko, M. Ohba and S. Kitagawa, *J. Am. Chem. Soc.*, 2007, **129**, 13706.
- (a) M.-H. Zeng, X.-L. Feng and X.-M. Chen, *Dalton Trans.*, 2004, 2217; (b) M. Nihei, L. Han and H. Oshio, *J. Am. Chem. Soc.*, 2007, **129**, 5312.
- (a) M. Kurmoo, H. Kumagai and K. W. Chapman, *Chem. Commun.*, 2005, 3012; (b) C.-L. Chen, A. M. Goforth, M. D. Smith, C.-Y. Su and zur H.-C. Loye, *Angew. Chem., Int. Ed.*, 2005, **44**, 6673.
- (a) P. Zhu, W. Gu, L.-Z. Zhang, X. Liu, J.-L. Tian and S.-P. Yan, *Eur. J. Inorg. Chem.*, 2008, 2971; (b) C. J. Kepert and M. J. Rosseinsky, *Chem. Commun.*, 1999, 375.
- (a) B. Rather and M. J. Zaworotko, *Chem. Commun.*, 2003, 830; (b) L. Dobrzańska, G. O. Lloyd, C. Esterhuysen and L. J. Barbour, *Angew. Chem., Int. Ed.*, 2006, **45**, 5856.
- (a) H. J. Park and M. P. Suh, *Chem.–Eur. J.*, 2008, **14**, 8812; (b) J. D. Ranford, J. J. Vittal and D. Wu, *Angew. Chem., Int. Ed.*, 1998, **37**, 1114.
- D.-X. Xue, W.-X. Zhang, X.-M. Chen and H.-Z. Wang, *Chem. Commun.*, 2008, 1551.
- (a) C. Hu and U. Englert, *Angew. Chem., Int. Ed.*, 2006, **45**, 3457; (b) H. Sadeghzadeh and A. Morsali, *Inorg. Chem.*, 2009, **48**, 10871.
- (a) S. Mishra, E. Jeanneau, S. Daniele and L. G. Hubert-Pfalzgraf, *CrystEngComm*, 2008, **10**, 814; (b) S. Mishra, E. Jeanneau, H. Chermette, S. Daniele and L. G. Hubert-Pfalzgraf, *Dalton Trans.*, 2008, 620.
- G. Mahmoudi and A. Morsali, *Cryst. Growth Des.*, 2008, **8**, 391.
- A. C. G. Hotze, Yu. Chen, T. W. Hambley, S. Parsons, N. A. Kratochwil, J. A. Parkinson, V. P. Munk and P. J. Sadler, *Eur. J. Inorg. Chem.*, 2002, 1035.
- V. T. Yilmaz, S. Hamamci, W. T. A. Harrison and C. Thöne, *Polyhedron*, 2005, **24**, 693.
- (a) T. I. A. Gerber, D. Luzipo and P. Mayer, *J. Coord. Chem.*, 2006, **59**, 1521; (b) C. Siaw-Lathey, H. Zhang and D. Y. Son, *Polyhedron*, 2005, **24**, 785; (c) C. Canada-Vilalta, E. Rumberger, E. K. Brechin, W. Wernsdorfer, K. Folting, E. R. Davidson, D. N. Hendrickson and G. Christou, *J. Chem. Soc., Dalton Trans.*, 2002, 4005; (d) S. Hamamci, V. T. Yilmaz and C. Thöne, *Acta Crystallogr., Sect. E: Struct. Rep. Online*, 2004, **60**, m159; (e) N. Lah, I. Leban and R. Clerac, *Eur. J. Inorg. Chem.*, 2006, 4888.
- R. S. Rowland and R. Taylor, *J. Phys. Chem.*, 1996, **100**, 7384.
- J. Grell, J. Bernstein and G. Tinhofer, *Acta Crystallogr., Sect. B: Struct. Sci.*, 1999, **55**, 1030.
- V. T. Yilmaz, S. Hamamci and C. Thöne, *Cryst. Res. Technol.*, 2002, **37**, 1143.
- G. M. Sheldrick, *Acta Crystallogr., Sect. A: Found. Crystallogr.*, 2008, **64**, 112–122.